Effect of Ionic Size on Solvate Stability of Glyme-Based Solvate Ionic Liquids

ARTICLE *in* THE JOURNAL OF PHYSICAL CHEMISTRY B · DECEMBER 2014

Impact Factor: 3.3 · DOI: 10.1021/jp508100s · Source: PubMed

8 AUTHORS, INCLUDING:

Toshihiko Mandai
Chalmers University of Technology
27 PUBLICATIONS **250** CITATIONS
SEE PROFILE

Hyuma Masu
Chiba University
132 PUBLICATIONS **1,346** CITATIONS
SEE PROFILE

Kazuhide Ueno
Yamaguchi University
69 PUBLICATIONS **1,244** CITATIONS
SEE PROFILE

Masayoshi Watanabe
Yokohama National University
350 PUBLICATIONS **14,344** CITATIONS
SEE PROFILE

THE JOURNAL OF PHYSICAL CHEMISTRY B

Article

pubs.acs.org/JPCB

Effect of Ionic Size on Solvate Stability of Glyme-Based Solvate Ionic Liquids

Toshihiko Mandai,[†,⊥] Kazuki Yoshida,[†] Seiji Tsuzuki,[‡] Risa Nozawa,[†] Hyuma Masu,[§] Kazuhide Ueno,[†] Kaoru Dokko,[†,∥] and Masayoshi Watanabe*[,†]

[†]Department of Chemistry and Biotechnology, Yokohama National University, 79-5 Tokiwadai, Hodogaya-ku, Yokohama 240-8501, Japan

[‡]National Institute of Advanced Industrial Science and Technology (AIST), Tsukuba Central 2, Tsukuba, Ibaraki 305-8568, Japan

[§]Center for Analytical Instrumentation, Chiba University, 1-33 Yayoi-cho, Inage-ku, Chiba 263-8522, Japan

[∥]Unit of Elements Strategy Initiative for Catalysts & Batteries (ESICB), Kyoto University, Kyoto 615-8510, Japan

Supporting Information

ABSTRACT: A series of binary mixtures composed of glymes (triglyme, G3; tetraglyme, G4; pentaglyme, G5) and alkali-metal bis(trifluoromethanesulfonyl)amide salts (M[TFSA]; M = Li, Na, and K) were prepared, and the correlation between the composition and solvate stability was systematically investigated. Their phase diagrams and Raman spectra suggested complexation of the glymes with M[TFSA] in 1:1 and/or 2:1 molar ratio(s). From isothermal stability measurements, it was found that the formation of structurally stable complexes in the solid state did not necessarily ensure their thermal stability in the liquid state, especially in the case of 2:1 complexes, where uncoordinating or highly exchangeable glyme ligands existed in the molten complexes. The phase-state-dependent Raman spectra also supported the presence of free glymes in certain liquid complexes. The effect of the electric field induced by the alkali-metal cations on the oxidative stability of certain glyme complexes was examined by linear sweep voltammetry and quantum chemical calculations. Although the actual oxidative stability of complexes did not necessarily reflect the calculated HOMO energy levels of the glymes, the strong electric field induced by the smaller M^+ cations and proper coordination structures impart high stability to the glyme complexes. The results of thermogravimetry of complexes with different M^+ cations revealed that a balance of competitive interactions of the M^+ ions with the glymes and $[TFSA]^-$ anions predominates the thermal stability.

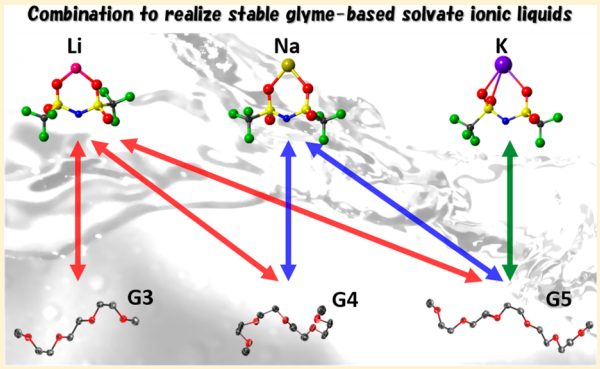

1. INTRODUCTION

Glymes (G*n*), which are oligoethers with CH_3O-$(CH_2CH_2O)_nCH_3$ structures, attract considerable interest as solvents for not only organic syntheses and extractions[1−4] but also electrolyte solutions containing various salts.[5−9] Because glymes have multiple ether-oxygen atoms with relatively high electron-donating abilities in each molecule, they undergo cooperative solvation that facilitates dissociation of salts. Their strong solvation abilities also impart remarkable features to the resulting electrolytes, such as chemical and electrochemical stability, low volatility, and high ionic concentration. Owing to these outstanding features, glyme−salt mixtures are one of the promising candidates for electrolytes for next-generation energy-storage devices, especially lithium−sulfur and lithium−air batteries.[6,8−15]

During our research into glyme−alkali metal salt systems, we found that only limited combinations of equimolar mixtures of glymes and alkali-metal salts (i.e., MX, where M and X are the parent cation and anion, respectively) form melt solvates, which consist of $[M(glyme)_1]^+$ and X^-, at ambient temperatures.[16−20] In these complexes, the M^+ cations strongly attract the lone-pair electrons of the ether-oxygen atoms within the glymes through ion−(induced) dipole interactions, thereby forming solvate cations. The resulting solvate cations behave as independent ions despite incorporating molecular solvents as ligands; hence, these molten mixtures can be regarded as solvate ionic liquids (ILs).[21] Among them, [Li(G3 or G4)$_1$][TFSA], which is an equimolar mixture of triglyme (G3) or tetraglyme (G4) with lithium bis(trifluoromethanesulfonyl)amide salt (Li[TFSA]), is one of the most representative solvate ILs.[22] From NMR measurements, the lifetimes of $[Li(G3 \text{ or } G4)_1]^+$ cations appear to be long enough to confirm that the Li^+ and coordinating glymes diffuse together.[18] Other experimental results have also proven

Received: August 10, 2014
Revised: November 11, 2014
Published: December 22, 2014

DOI: 10.1021/jp508100s
J. Phys. Chem. B 2015, 119, 1523−1534

that their features are comparable to those of conventional ILs, and include low volatility and flammability and high ionic conductivity.[16,18] On the basis of these remarkable properties, we extend our study to the use of solvate ILs as new electrolytes for a variety of Li and Na secondary batteries.[12,23−28]

Preceding our research, several researchers also took interest in the concentrated glyme−Li salt systems. It was pointed out that highly concentrated glyme mixtures with Li[TFSA] form amorphous liquids at ambient temperature in 1998.[29] Phase behaviors of these systems incorporating different glymes and Li salts were extensively studied,[29−34] and low melting equimolar complexes, which should be classified as solvate ionic liquids, have been found.[29−35] In addition to the studies on phase behavior, physicochemical properties of the concentrated mixtures were also investigated. NMR dynamics and electrochemical studies clarified the remarkable characteristics in Li^+ ion diffusion mechanism and electrochemical stability especially for the highly concentrated mixtures.[35,36]

Ion−ion and ion−solvent interactions are complicated in such extremely concentrated electrolyte systems. For the glyme−MX mixtures, the cation−dipole interactions between M^+ and glymes compete with the cation−anion interactions between M^+ and X^-; this competition strongly affects the structures and properties of the resulting complexes. For example, the solvate structures of G1−G4 with different Li salts depend on both the glyme length and counteranionic structures even though either the former or latter structure is fixed,[30−34,37−39] as was demonstrated by pioneering work by Henderson et al.[31−34] Binary mixtures consisting of $LiAsF_6$ and longer glymes (G8−12) form distinct structures in the crystalline state depending on their composition.[40] In addition to the solvate structures, the glyme length (i.e., the chelate effect) and anionic structure also significantly impact the stability of the complex cation, $[Li(glyme)]^+$, in molten complexes.[19,22,41,42] The structural stability of complex cations plays an important role in the performance of Li batteries.[43] Long-lived stable complex cations can be achieved in the few cases where the interactions between the Li^+ cations and glymes with strong chelating abilities overwhelm the interactions between the Li^+ cations and anions.

Likewise, the cationic metal species (M^+) also affect both the structures and properties of the complexes. In our previous work, we scrutinized a series of glyme−NaX complexes with respect to their phase diagrams, solvate structures, and physicochemical properties.[20] However, the effect of the ionic size in $[M(glyme)_1]X$ (M = Li, Na, and K) complexes on the solvate stability has yet to be clarified. To this end, we study herein the correlation between composition and solvate stability for a series of binary mixtures composed of different glymes and M[TFSA] salts (M = Li, Na, and K). It is well-known that Li^+, Na^+, and K^+ cations possess large complex-formation constants with 12-crown-4, 15-crown-5, and 18-crown-6 ethers, respectively.[44,45] On the basis of such coordination chemistry, G3, G4, and pentaglyme (G5) were selected as ligand molecules because their chemical structures in the coordination state are similar to those of the corresponding crown ethers. In this study, from phase diagrams and Raman spectra, the compositions that form structurally stable complexes are explored. The coordination structures in both crystalline and liquid states are evaluated via single-crystal structures and phase-state-dependent Raman spectra. From the obtained coordination structures of the solvates, we study the effect of ionic size on electrochemical and thermal stabilities using linear sweep voltammetry and thermogravimetry, respectively, with the help of quantum mechanical calculations.

2. EXPERIMENTAL SECTION

2.1. Materials. Li[TFSA] was purchased from Morita Chemical Industries Co., Ltd. H[TFSA], Na_2CO_3, G3, and G4 were obtained from Tokyo Chemical Industry Co., Ltd. G5 was kindly supplied by Nippon Nyukazai and used as received. 1,1,2,2-Tetrafluoroethyl-2,2,3,3-tetrafluoropropyl ether (HFE), which is a recrystallization solvent for complexes, was purchased from Daikin Industries. K[TFSA], potassium hexafluorophosphate (KPF_6), 12-crown-4, 15-crown-5, and 18-crown-6 ethers, and other chemicals were purchased from Wako Chemical. G3 and G4 were distilled under high vacuum over sodium metal. Hexaglyme (G6) was synthesized according to the Williamson reaction using tetraethylene glycol and 2-methoxyethanol. Owing to the high boiling point and low vapor pressure of G6, column chromatography was performed twice to purify it, followed by treatment with molecular sieves 4A. The residual water contents in these glymes, as measured by Karl Fischer titration, were less than 50 ppm. Na[TFSA] was synthesized by neutralization of H[TFSA] and Na_2CO_3 according to a previously published procedure.[20,46] All the salts were dried under high vacuum at 80 °C for 36 h and stored in an Ar-filled glovebox for use. A series of glyme−M[TFSA] binary mixtures, i.e., $[M(glyme)_n][TFSA]$, were prepared by mixing stoichiometric salts and glymes in an Ar-filled glovebox. $[K(G4)_2]PF_6$, $[K(G5)_1]PF_6$, and $[K(G6)_1]PF_6$ were also prepared by mixing appropriate amounts of KPF_6 and each glyme. To achieve complete mixing during sample preparation, the mixtures were heated to 80 °C and stirred for 3 days. Equimolar mixtures of crown ethers (12-crown-4, 12C4; 15-crown-5, 15C5; and 18-crown-6, 18C6) and M[TFSA] were also obtained by mixing in the glovebox. These crown-ether-based complexes were prepared upon the addition of parent salts into the crown ether/acetone solution, followed by removal of the solvent under vacuum.

2.2. Measurements. The phase behaviors of all mixtures were evaluated using a differential scanning calorimeter (DSC 6220 or DSC7020; Seiko). The samples were hermetically sealed in aluminum pans in the glovebox. A scanning rate of 5 or 10 °C min^{-1} and a measured temperature range from −150 to 100 °C (150 °C if necessary) under a nitrogen atmosphere were employed. The sample pans were repeatedly cooled/annealed to achieve complete crystallization of the complexes. The peak tops of the corresponding endothermic peaks were used to determine the melting points (T_m) and other thermal transition temperatures (T_x), and the onset in heat capacity change was defined as the T_g. Thermogravimetric (TG) measurements were performed on a TG/TDA 6200 instrument (Seiko) to estimate the thermal stabilities of the studied mixtures. The samples were heated from room temperature to 550 °C at a heating rate of 10 °C min^{-1}. The isothermal stabilities of the samples were evaluated by monitoring the weight loss of samples held at 100 °C for 3 h.

The electrochemical stabilities of selected $[M(glyme)_1]$-[TFSA] complexes were evaluated by linear sweep voltammetry (LSV) using an electrochemical analyzer (Princeton Applied Research, VMP3) and a three-electrode cell with a scan rate of 1 mV s^{-1} at 60 °C. A platinum electrode was used as the working and counter electrodes, and the reference electrode consisted of a Li metal foil soaked in $[Li(G4)_4][TFSA]$ confined in a glass tube equipped with a liquid junction.

DOI: 10.1021/jp508100s
J. Phys. Chem. B 2015, 119, 1523−1534

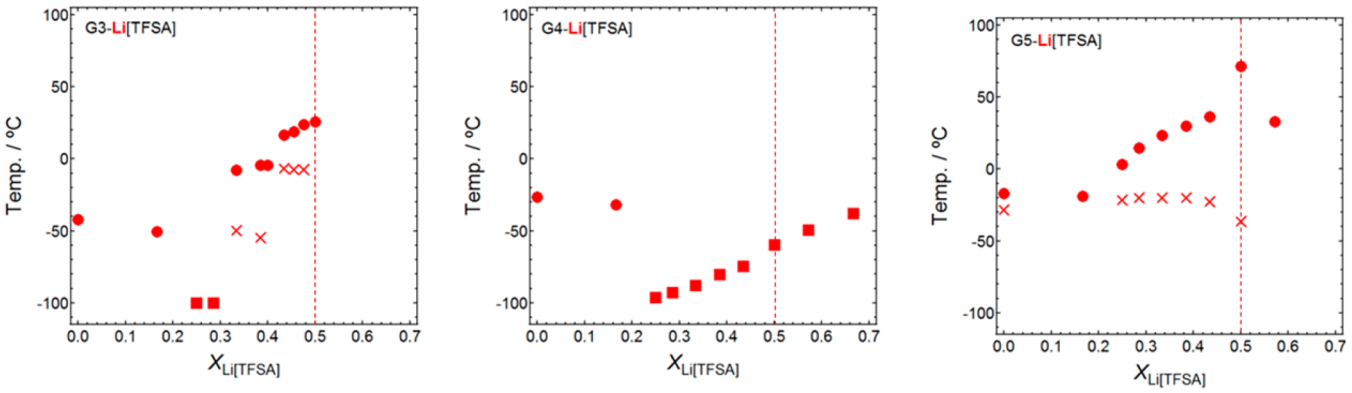

Figure 1. Phase diagrams of the G3−Li[TFSA] (left), G4−Li[TFSA] (center), and G5−Li[TFSA] (right) systems as a function of the mole fraction of Li[TFSA]. The dotted line in each figure indicates the composition at which the stoichiometric complex is formed. Closed circles, T_m; closed squares, T_g; crosses, T_x.

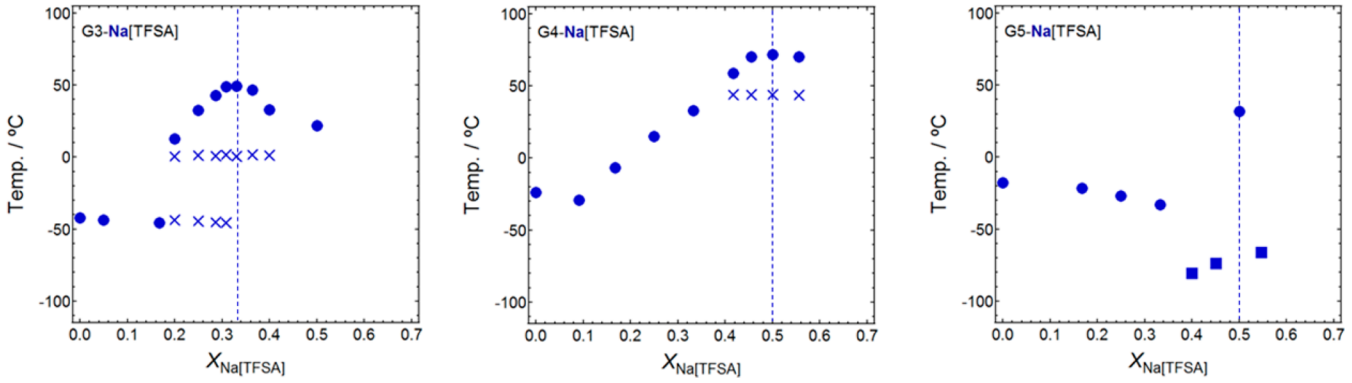

Figure 2. Phase diagrams of the G3−Na[TFSA] (left), G4−Na[TFSA] (center), and G5−Na[TFSA] (right) systems as a function of the mole fraction of Na[TFSA]. The dotted line in each figure indicates the composition at which the stoichiometric complex is formed. Closed circles, T_m; closed squares, T_g; crosses, T_x.

Raman spectra were measured using a portable Raman system (RMP-330, Jasco) and the 532 nm line of an LD-excited solid laser with a resolution of ∼2 cm^{-1}. Raman spectra of the studied mixtures were measured in the range 1000−500 cm^{-1} at ambient temperature (23 ± 2 °C). For certain equimolar complexes, the Raman spectra were measured at elevated temperatures to examine the coordination environment of the complexes in the liquid state using a hot stage with a temperature controller (mK1000; Instec). To analyze the representative Raman shifts and wave shapes, suitable spectral ranges were adopted: 900−780 and 760−720 cm^{-1} for glyme and $[TFSA]^-$, respectively.

X-ray crystallography was performed on $[Li(G5)_1][TFSA]$, $[K(G5)_1][TFSA]$, $[Li(12C4)_1][TFSA]$, $[K(18C6)_1][TFSA]$, $[K(G4)_2]PF_6$, $[K(G5)_1]PF_6$, and $[K(G6)_1]PF_6$. Excepting $[Li(G5)_1][TFSA]$, suitable crystals were obtained by slow condensation of concentrated acetone or HFE solutions. A suitable crystal of $[Li(G5)_1][TFSA]$ was obtained from a 1:2 mixture of Li[TFSA] and G5. Each single crystal was mounted on a glass pin and cooled to −100 or −50 °C using a stream of nitrogen gas. Crystallographic data collections were performed on a CCD detector with monochromated Mo Kα (λ = 0.710 73 Å) or Cu Kα (λ = 1.541 78 Å) radiation. The structures were solved using direct methods, i.e., SIR92[47] or SHELEXS-97, and refined using full-matrix least-squares SHELXL-97.[48,49] Non-hydrogen atoms were refined anisotropically, and hydrogen atoms were included in their ideal position. The crystallographic data and solvate models for the solved structures are included in Supporting Information (Table S1 and Figures S1−S7).

2.3. Calculations. The Gaussian 03 program[50] was used for the ab initio molecular orbital calculations. The geometries of the ion pairs and certain complexes were fully optimized at the HF/6-311G** level. The highest occupied molecular orbital (HOMO) energy levels were calculated at the HF/6-311G** level using the fully optimized geometries.

3. RESULTS AND DISCUSSION

3.1. Structural Aspects of Solvate Ionic Liquids. *Phase Behavior.* The phase diagrams of a series of glyme−M[TFSA] mixtures are summarized in Figures 1−3. The results for the G4− and G5−Na[TFSA] systems are reproduced from ref 20. Because of their low miscibility, the G3−K[TFSA] mixtures are not investigated. As shown in the figures, the phase diagrams clearly illustrate features characteristic of complex formation that depend on both the metal ion species and glyme length.

For the glyme−Li[TFSA] systems (Figure 1), T_m maxima are observed at a 1:1 molar ratio, except for G4−Li[TFSA]. These results suggest that equimolar complexes of Li[TFSA] with G3 or G5 are formed. Additional thermal transitions are also observed before melting for these systems, suggesting the presence of intermediate phases other than equimolar phases or solid−solid phase transitions; they are plotted as T_x. In contrast, G4−Li[TFSA] mixtures are liable to form glasses over the wide composition range of $0.25 \leq x \leq 0.67$. This observation is consistent with the preceding works done by

DOI: 10.1021/jp508100s
J. Phys. Chem. B 2015, 119, 1523−1534

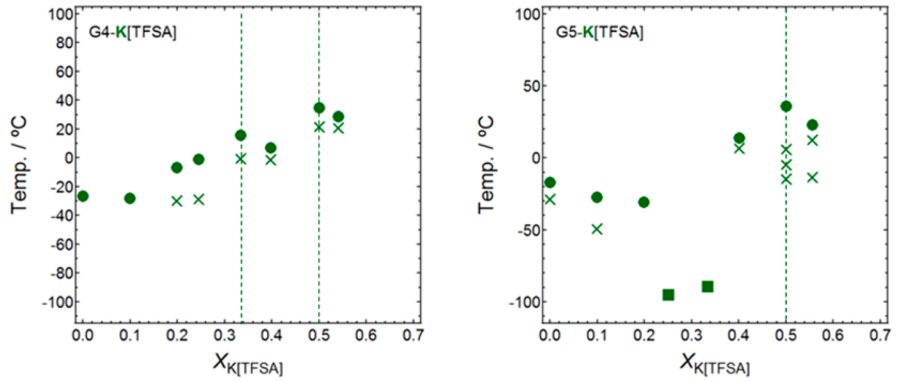

Figure 3. Phase diagrams of the G4−K[TFSA] (left) and G5−K[TFSA] (right) systems as a function of the mole fraction of K[TFSA]. The dotted lines indicate the compositions at which stoichiometric complexes are formed. Closed circles, T_m; closed squares, T_g; crosses, T_x.

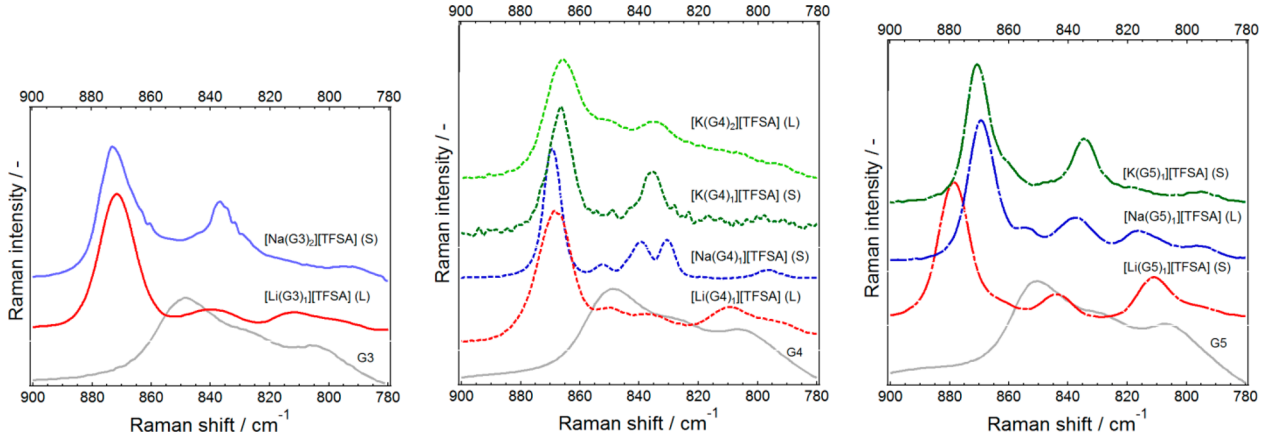

Figure 4. Selected Raman spectra for a series of [M(glyme)$_n$][TFSA] complexes at ambient temperature. "S" and "L" in each label indicate the solid and liquid states, respectively.

Brouillette and Henderson.[30,31] Unfortunately, crystallization of [Li(G4)$_1$][TFSA] (x = 0.5) has not yet been accomplished; however, its optimized structure was calculated.[18,51] In that structure, four oxygen atoms within G4 coordinate to a Li^+ ion, while the last oxygen atom does not participate in coordination; this situation leads to high conformational flexibility of the coordinating G4 molecules and consequently prevents crystallization of the complex.

In the case of the glyme−Na[TFSA] mixtures (Figure 2), the phase behavior is also dependent on the glyme length. For the G4−Na[TFSA] mixtures, the T_m maximum at a 1:1 molar ratio clearly indicates complexation at the equimolar composition. For the G5−Na[TFSA] mixtures, it is not clear if the T_m observed at the 1:1 composition is a local maximum because of the crystallinity gap at the Na[TFSA] composition around x = 0.5, where only a glass transition is observed. However, the observation of a single melting peak at the 1:1 molar ratio implies the formation of a single complex.[20] In contrast, the G3−Na[TFSA] mixture shows a T_m maximum at x = 0.33, which suggests complexation at a 2:1 molar ratio.

As in the case of the G3−Na[TFSA] system, the diagram of G4−K[TFSA] indicates 2:1 complex formation. Interestingly, two local T_m maxima are observed at x = 0.33 and 0.5, which implies the formation of both 2:1 and 1:1 complexes (Figure 3). A similar complexation behavior was reported for the binary mixture of G2 and Li[TFSA], where crystal structures of 2:1 and 0.5:1 complexes were obtained.[31]

With respect to the correlation between the metal ions and phase behavior, characteristic features are extracted. The glyme length that enables 1:1 complex formation increases with increasing metal ion size; i.e., Li, Na, and K prefer complexation with Li ≥ G3, Na ≥ G4, and K ≥ G5, respectively. A similar trend is evident for 2:1 complexes: Li, Na, and K salts require complexation with two equivalents of G2, G3, and G4, respectively. These phenomena can be attributed to the ionic radii and coordination number of each metal ion, and are discussed in detail below.

Complexation and Stability. Complexation of glymes with M[TFSA] can be confirmed by Raman spectroscopy. It is well-known that a characteristic Raman band, which is known as the ring-breathing mode, is observed at ∼870 cm^{-1} when these binary mixtures form crown-ether-like complexes (Supporting Information, Figure S8).[20,30,37] Hence, this band is known as one of the fingerprints of complex formation. Raman spectra were measured for the mixtures that exhibited local maxima of T_m in their phase diagrams, as shown in Figure 4. The spectra of pure glymes are also included in Figure 4. The breathing mode is clearly evident in all the studied spectra, indicating complexation between the glymes and M[TFSA] in 1:1 and/or 2:1 molar ratios. In the liquid [K(G4)$_2$][TFSA] spectrum, a broad peak or shoulder appears at ∼850 cm^{-1}, which corresponds to the vibrational mode of pure glymes. This result suggests the presence of free or highly exchangeable glyme molecules in this molten mixture.

DOI: 10.1021/jp508100s
J. Phys. Chem. B 2015, 119, 1523−1534

The isothermal stabilities of the molten complexes are another indicator of the formation of stable glyme−M[TFSA] complexes in the liquid state because complexation with metal ions suppresses the evaporation of glymes.[16,17,20] Figure 5

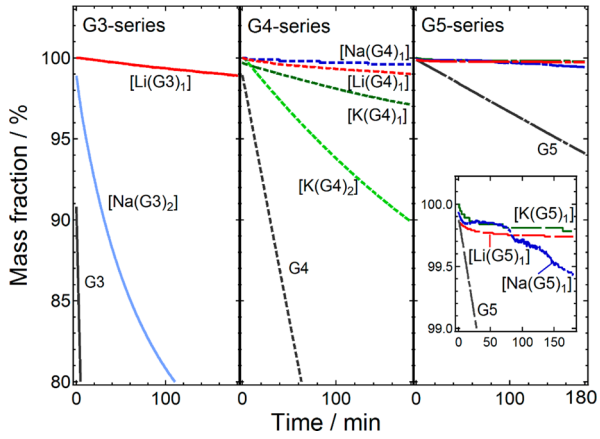

Figure 5. Isothermal TG curves of selected $[M(glyme)_n][TFSA]$ complexes at 100 °C for 3 h. Curves of pure glymes are also included. The red, blue, green, and gray lines indicate the curves of $[Li(glyme)_1][TFSA]$, $[Na(glyme)_n][TFSA]$, $[K(glyme)_n][TFSA]$, and the pure glymes, respectively. Inset is the magnification of the curves of the G5 series.

shows isothermal TG curves (100 °C for 3 h) of the binary mixtures, which form complexes as indicated by the phase diagrams (Figures 1−3) and Raman spectra (Figure 4). Negligible weight loss is evident in the $[Li(glyme)_1][TFSA]$ curves irrespective of the glyme length, which implies strong complexation of the Li^+ ions with the glymes. In contrast, the isothermal stabilities of the complexes involving Na[TFSA] and K[TFSA] were glyme-length-dependent. For $[Na(G3)_2]$-[TFSA], evaporation of uncoordinating or highly exchangeable (i.e., weakly coordinating) G3 molecules occurs, whereas its Raman spectrum and phase diagram suggest the presence of a 2:1 phase. In contrast, the isothermal TG results of $[Na(G4)_1][TFSA]$ and $[Na(G5)_1][TFSA]$ clearly demonstrate their high stability. Likewise, an apparent weight loss due to evaporation of glymes is observed for $[K(G4)_2][TFSA]$ and $[K(G4)_1][TFSA]$, while $[K(G5)_1][TFSA]$ possesses sufficient stability at 100 °C. These results enable us to propose the basic requirements for thermally stable molten glyme−M[TFSA] complexes: (1) the mixture should form a complex in a 1:1 molar ratio and (2) the glymes should be the appropriate length for the alkali-metal cations.

As stated before, Li^+, Na^+, and K^+ ions have high affinities for 12-crown-4, 15-crown-5, and 18-crown-6 ethers, respectively.[44] Complexation with a smaller ligand (for example, a Na^+ ion with 12-crown-4 ether) usually requires coordination by two equivalents of the ligands.[52−55] G3, G4, and G5 contain four, five, and six oxygen atoms, respectively; accordingly, G3−Na[TFSA] and G4−K[TFSA] mixtures tend to form complexes in 2:1 ratios. A similar result was seen in the binary mixture of G2 and Li[TFSA], which forms $[Li(G2)_2][TFSA]$.[31] It should be noted here that the binary mixture of 12-crown-4 ether and Li[TFSA] tends to form not only a 1:1 complex but also a 2:1 complex, $[Li(12C4)_2][TFSA]$;[56] nevertheless, crystal structures of the corresponding glyme-based 2:1 complexes, $[Li(G3)_2]X$, have never been reported. Preferential coordination number of Li^+ ion, steric effect of neighboring glymes, and slow crystallization kinetics probably inhibit crystallization.[34] On the other hand, this 2:1 complex formation in glyme−solvate systems is independent of the anionic structure.[34] In fact, the binary mixture of G4 and KPF_6 also forms a 2:1 complex (vide infra). The relatively low stability of 2:1 complexes can be interpreted based on their structural features: 2:1 complex formation increases the steric hindrance and relaxation of positive charge density, which leads to weaker ion−dipole interactions of the M^+ ion with a single glyme than in 1:1 complexes. Actually, the distances between K^+ and the oxygen atoms ($K-O_{glyme}$) of $[K(G4)_2]PF_6$ (2.86−3.07 Å) are longer than those of $[K(G5)_1]PF_6$ (2.82−2.91 Å) (see Supporting Information, Table S2). Therefore, the weak ion−dipole interactions probably cause the relatively low thermal stability of 2:1 complexes.

Coordination Structures in Crystalline and Liquid States. Single-crystal structures of $[Na(G4)_1][TFSA]$ and $[Na(G5)_1]$-[TFSA] have already been reported.[20] In addition to these complexes, the crystal structures of $[Li(G5)_1][TFSA]$ and $[K(G5)_1][TFSA]$ are reported here. Due to their low crystallinity, which originates from the conformational flexibility of the components, crystal structures of glyme−Li[TFSA] involving G3 and G4 have not been obtained. Henderson et al. reported the crystal structure of $[Li(G3)_1][BETA]$ (BETA, bis(pentafluoroethylsulfonyl)amide).[31] Because of the structural analogy between $[TFSA]^-$ and $[BETA]^-$ anions, the solvate structure of $[Li(G3)_1][TFSA]$ is suggested to be similar to that of $[Li(G3)_1][BETA]$. For comparison, structures of the corresponding crown-ether-based complexes, such as $[Li(12C4)_1][TFSA]$, $[Na(15C5)_1][TFSA]$, and $[K(18C6)_1]$-[TFSA], are also investigated.

In the $[M(glyme)_1][TFSA]$ crystals, glyme molecules wrap around each M^+ ion with a characteristic coordination framework, as is seen in the corresponding crown-ether-based complex. The counter $[TFSA]^-$ anions also coordinate to M^+ ions in monodentate or bidentate forms depending on the compositions, resulting in CIP-I (contact ion pair with a monodentate anion) or AGG (aggregate) type solvates, respectively, with the exception of $[Li(G5)_1][TFSA]$. Although the crystal structures of both $[Li(G3)_1][BETA]$ and $[Na(G5)_1][TFSA]$ belong to CIP-I type solvates, the manners of coordination of the glymes are slightly different. G3 coordinates to the Li^+ ion to form a complex cation $[Li(G3)_1]^+$ analogous to $[Li(12C4)_1]^+$ (Supporting Information, Figure S3), whereas G5 and Na^+ ions form characteristic complex cations $[Na(G5)_1]^+$.[20,28] A similar coordination manner of glyme to that in $[Na(G5)_1]^+$ is also observed in the crystal structure of $[K(G6)_1]PF_6$ (Supporting Information, Figure S7). In these crystals, one oxygen atom within a terminal ethylene oxide (EO) unit coordinates to a M^+ ion from the foreside of the crown-like plane constructed by the other (four or five) EO units. These characteristic structures also prove the high affinity of each M^+ ion with appropriate ether-based ligands. On the other hand, in both $[Na(G4)_1][TFSA]$ and $[K(G5)_1][TFSA]$ crystals, glymes wrap around each metal ion, as seen in the corresponding crown-ether-based counterparts; these solvates are classified as AGG. Two oxygen atoms within a $[TFSA]^-$ anion coordinate to two different M^+ cations as bridging agents resulting in one-dimensionally aligned structures.

Structural specificity can also be seen in the crystal structure of $[Li(G5)_1][TFSA]$ (Supporting Information, Figure S1). In this solvate, the G5 molecule wraps tightly around the Li^+ cation and all six oxygen atoms within a single G5 molecule

DOI: 10.1021/jp508100s
J. Phys. Chem. B 2015, 119, 1523−1534

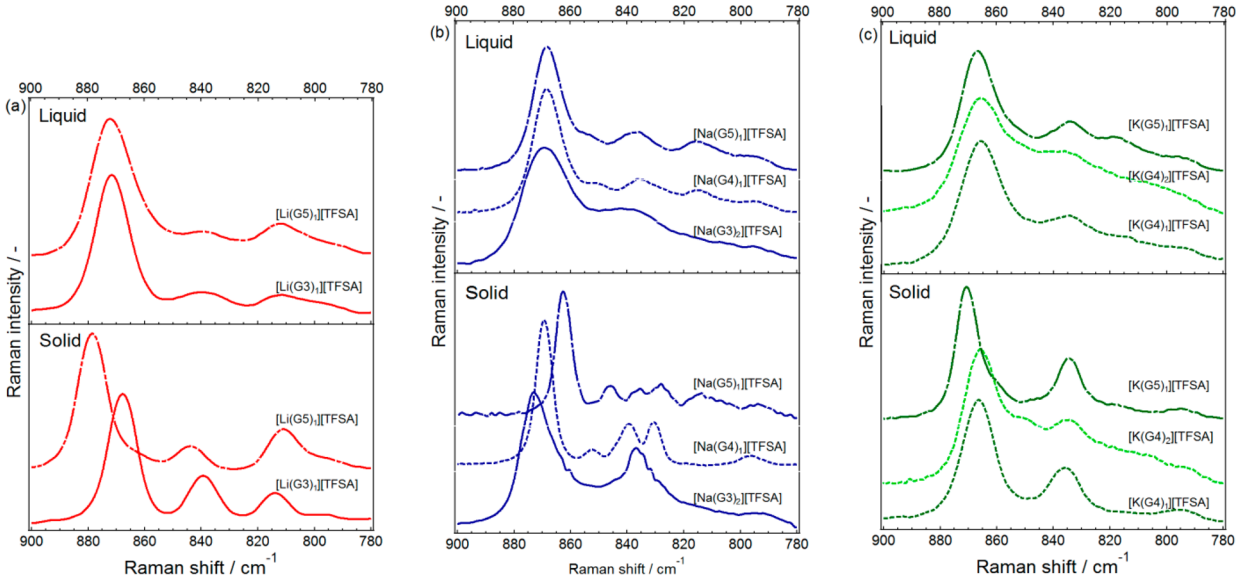

Figure 6. Phase-state-dependent cationic Raman spectra of selected $[M(glyme)_n][TFSA]$ complexes: (a) $[Li(glyme)_1][TFSA]$, (b) $[Na(glyme)_n][TFSA]$, and (c) $[K(glyme)_n][TFSA]$.

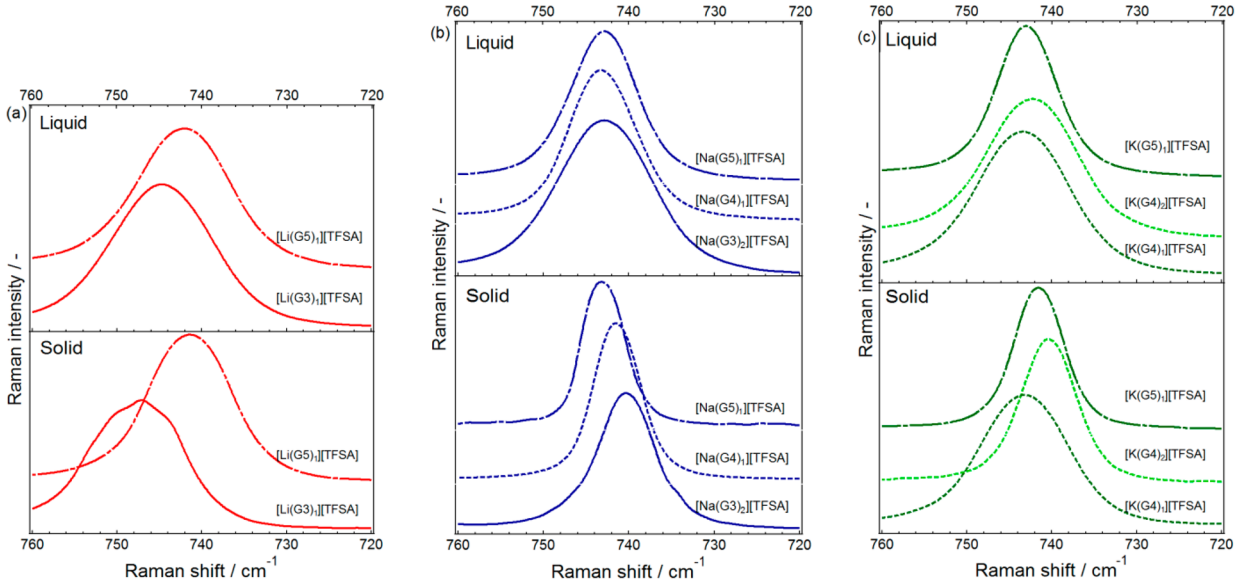

Figure 7. Phase-state-dependent anionic Raman spectra for selected $[M(glyme)_n][TFSA]$ complexes: (a) $[Li(glyme)_1][TFSA]$, (b) $[Na(glyme)_n][TFSA]$, and (c) $[K(glyme)_n][TFSA]$.

coordinate to the Li^+ cation. The $[TFSA]^-$ anion does not participate in coordination to the Li^+ cation resulting in the formation of a solvent-separated ion pair (SSIP) type solvate. This solvate closely resembles $[Li(G2)_2][TFSA]$ in the coordination structure and solvate type: The hexacoordinated Li^+ cation is coordinated by two G2 molecules to form an SSIP-type solvate in the crystalline state.[31] Their Raman spectra also demonstrate the structural similarities between $[Li(G5)_1]$-$[TFSA]$ and $[Li(G2)_2][TFSA]$, as shown in Figure 4 and the Supporting Information, Figure S9.

Unfortunately, the crystal structures of $[Na(G3)_2][TFSA]$ and $[K(G4)_2][TFSA]$ have not been clarified because of their low crystallinity and crystal polymorphism. However, we can estimate them from other structures. Single-crystal X-ray crystallography of $[K(G4)_2]PF_6$ revealed that the K^+ cation is coordinated by 10 oxygen atoms from two G4 molecules resulting in a decacoordinated SSIP solvate (Supporting Information, Figure S5). Owing to the structural resemblance between $[K(G5)_1][TFSA]$ and $[K(G5)_1]PF_6$ (Supporting Information, Figures S2 and S6), crystalline $[K(G4)_2][TFSA]$ would form an SSIP-type solvate analogous to $[K(G4)_2]PF_6$. Similarly, it has been reported that the crystalline $[Na(G3)_2]$-[biphenylene] solvate is an SSIP-type solvate.[57] In addition, as stated before, the binary mixture of G2 and Li[TFSA] forms a 2:1 phase, which is also classified as an SSIP-type solvate.[31] According to these structural characteristics, it is strongly suggested that the 2:1 complexes composed of short glymes and alkali-metal salts are likely to form SSIP-type solvates. The preferential coordination number of the metal ions and molar ratio of the metal ions and ether-oxygen atoms ($[O]/[M^+]$) in each solvate are closely related to this structural feature. Actually, $[Li(G1)_3][TFSA]$ ($[O]/[Li^+] = 6$) is suggested to

DOI: 10.1021/jp508100s
J. Phys. Chem. B 2015, 119, 1523−1534

form an SSIP-type solvate,[34] whereas $[Li(G1)_2]ClO_4$ ($[O]/[Li^+] = 4$) is a CIP.[58]

Interestingly, the results of crystallography on these glyme-based complexes suggest minimum requirements for the coordination number of each metal ion in the crystalline state, i.e., $Li^+ \geq 5$, $Na^+ \geq 7$, $K^+ \geq 8$. For example, Li^+ ions are coordinated by five and six oxygen atoms in $[Li(G3)_1][BETA]$ and $[Li(G2)_2][TFSA]$, respectively.[31] The coordination number of Li^+ ions in $[Li(G3)_1][X]$ solvates (polymerized AGG-type solvates in the form of $[Li_n(G3)_n][X]_n$) paired with other anions, such as $X = CF_3SO_3^-$, ClO_4^-, and AsF_6^-, is five.[32] In the case of the other cations, hepta- and octacoordinated Na^+ ions and octa- to decacoordinated K^+ ions have been reported.[20] The cause of the 2:1 complex formation can be proposed from the above requirement: The coordination number of each metal ion should at least satisfy the specified coordination. It should be noted that this requirement can only be applied to these glyme-based systems; as an example, tetracoordinated lithium solvates have been reported for mixtures of Li salts with other monodentate ligands, such as acetonitrile, tetrahydrofuran, and ethylene carbonate.[59−63]

The coordination structure in the liquid state can be estimated from Raman spectra of the liquid and crystalline states together with the corresponding crystal structures. As stated above, the breathing mode observed at ∼870 cm^{-1} is the fingerprint for complex formation. In addition, the Raman active expansion−contraction modes of the entire anion, which appear at ∼740 cm^{-1}, are particularly sensitive to changes in the environment of the anions.[64] Using these bands as a probe, we can examine the coordination structures of a series of glyme−M[TFSA] complexes (mixtures) in the liquid state. The liquid-state spectra were collected at 15 °C above the T_m of each complex.

Cationic and anionic Raman spectra of the crystalline and liquid states of $[M(glyme)_n][TFSA]$ are shown in Figures 6 and 7, respectively. The spectra for $[Na(G4)_1][TFSA]$ and $[Na(G5)_1][TFSA]$ are reproduced from ref 20. The $[Li(G4)_1]$-[TFSA] spectrum is excluded because it keeps the liquid state under the measured conditions. Variation of their spectra upon phase transition demonstrates the solvate stability; these results are consistent with the isothermal stability measurements. As shown in Figure 6, broad peaks assigned to free glymes emerge in the spectra of $[Na(G3)_2][TFSA]$, $[K(G4)_1][TFSA]$, and $[K(G4)_2][TFSA]$ and indicate desolvation of the glymes from their complex cation structures upon melting. Spectral variation is also observed in the phase-state-dependent $[Li(G2)_2][TFSA]$ spectra (Supporting Information, Figure S9). In contrast, similar cationic spectra are observed for the other complexes irrespective of the phase state. Variation of the relative intensity between the free and coordinating glymes elucidates the generation of free glymes through solid−liquid phase transition. As shown in the Supporting Information, Figure S10, the relative intensity of the peak assigned to free glymes (i.e., the broad peak at ∼850 cm^{-1}) increases considerably upon melting for $[Na(G3)_2][TFSA]$, $[K(G4)_1][TFSA]$, and $[K(G4)_2]$-[TFSA], whereas that intensity is independent of the phase state for the other equimolar complexes. These results also support the high stability of the 1:1 complexes.

Anionic spectra also impart important information on the coordination structures of complexes. The expansion−contraction band frequencies in both crystalline and liquid states are listed in Table 1. It should be noted that the representative expansion−contraction bands observed at ∼741 and 743 cm^{-1} are due to the bidentate (bridging) and monodentate $[TFSA]^-$ anions, respectively, for complexes involving Na[TFSA] or K[TFSA].[20] In the case of Li[TFSA] solvates, free or SSIP $[TFSA]^-$ anions are characterized by a band at ∼739−742 cm^{-1}; CIP- and AGG-type solvates produce this band at higher frequencies (typically ≥744 cm^{-1}).[30,64,65] As listed in Table 1, the physical state does not affect the anionic band frequencies for $[Li(G5)_1][TFSA]$ and $[Na(G5)_1][TFSA]$, suggesting that $[TFSA]^-$ anions coordinate to the metal ions similarly in the crystalline and liquid states (SSIP for the former and CIP for the latter). On the other hand, these bands for the other complexes, except $[Li(G3)_1][TFSA]$, shift to a higher frequency upon melting. Among them, the bands in the spectra of $[Na(G4)_1][TFSA]$ and $[K(G5)_1][TFSA]$ observed at 741 cm^{-1} in the crystalline state shift to 743 cm^{-1} in the liquid state; the resultant band frequency is consistent with that of $[Na(G5)_1][TFSA]$. The $[TFSA]^-$ anions in $[Na(G5)_1]$-[TFSA] coordinate to the Na^+ ions in a monodentate form, resulting in the formation of CIP-type solvates. In addition, the glymes still coordinate to Na^+ or K^+ ions, thereby forming $[Na(G4)_1]^+$ and $[K(G5)_1]^+$ complex cations even in the liquid state, as confirmed by the phase-state-dependent cationic spectra (Figure 6). Therefore, the AGG structures of $[Na(G4)_1][TFSA]$ and $[K(G5)_1][TFSA]$ in the crystalline state break upon melting and form CIP-type solvates in the liquid state. Both cationic and anionic spectra (specifically the frequencies of the breathing and expansion−contraction modes, respectively) change considerably upon melting, especially for the 2:1 complexes. These spectral variations strongly suggest that, although the $[TFSA]^-$ anions are separated from the solvate cations to form SSIP-type solvates in the crystalline state, they coordinate to the metal ions upon decomposition of the cationic solvate structures. The spectral results also verify the structural instability of these complexes. Furthermore, a peculiar shift of expansion−contraction band frequency is observed for $[Li(G3)_1][TFSA]$: The band shifts to a lower frequency upon melting (from 747 to 744 cm^{-1}). As stated before, both bands are assigned to the formation of CIP- or AGG-type solvates, i.e., $[TFSA]^-$ anions coordinating to Li^+ ions; however, the shift to a lower frequency indicates fading of ion−ion interactions. The increased mobility of the ions after melting probably causes this phenomenon.

As mentioned above, the stability of the mixtures in the molten states is strongly influenced by the composition even though they evidently form complexes at certain molar ratios in the solid state. Almost all 1:1 complexes are relatively stable; however, complexation of M^+ ions with two equivalent glymes results in unstable 2:1 complexes. On the basis of the criteria for solvate ILs, which were proposed in our previous paper,[22]

Table 1. Selected Vibrational-Frequency Variations for $[TFSA]^-$ Anions upon Melting

	Raman shift/cm^{-1}	
sample	crystal	liquid
$[Li(G3)_1][TFSA]$	747	744
$[Li(G5)_1][TFSA]$	741	742
$[Na(G3)_2][TFSA]$	740	743
$[Na(G4)_1][TFSA]$	741	743
$[Na(G5)_1][TFSA]$	743	743
$[K(G4)_1][TFSA]$	743	743
$[K(G4)_2][TFSA]$	740	742
$[K(G5)_1][TFSA]$	741	743

DOI: 10.1021/jp508100s
J. Phys. Chem. B 2015, 119, 1523−1534

equimolar complexes with high stability can be regarded as good solvate ILs. In contrast, 2:1 complexes only partially satisfy the criteria, which indicates that they are categorized into poor solvate ILs. The differences between good and poor solvate ILs emerge clearly in their structural stability in the liquid state.

3.2. Ionic-Size Effect on the Electrochemical and Thermal Stabilities of Complexes. Glyme molecules coordinating to M^+ are highly polarized by the strong electric field of the metal ions, resulting in lowering of its HOMO energy level. Electrochemical oxidation of glyme molecules at the electrode/electrolyte interface occurs when electrons are extracted from the HOMO of glyme; thus, a lower HOMO energy level leads to higher oxidative stability. The magnitude of the electric-field effect correlates strongly with the metal ion size. On the other hand, weight loss in temperature-dependent thermogravimetry below 400 °C is attributed to evaporation of glymes. Strong ion−(induced) dipole (M^+−glyme) interactions suppress desolvation of coordinating glymes, hence make complexes thermally stable. Because the M^+−glyme interaction is also influenced by the positive charge density of the metal ions, the electric-field effect (induction interaction) and ion−dipole interaction (electrostatic interaction) are mutually correlated. In this section, we will discuss the electrochemical and thermal stabilities of glyme−M[TFSA] solvate ILs with respect to the electric-field effect and ion−dipole interactions with the help of quantum mechanical calculations.

Electrochemical Stability. The stabilities of the complexes toward electrochemical oxidation were assessed using linear sweep voltammetry (LSV). Because certain complexes are solid at ambient temperatures, the measurements were performed at 60 °C. The LSV results are summarized in Figure 8. Typical

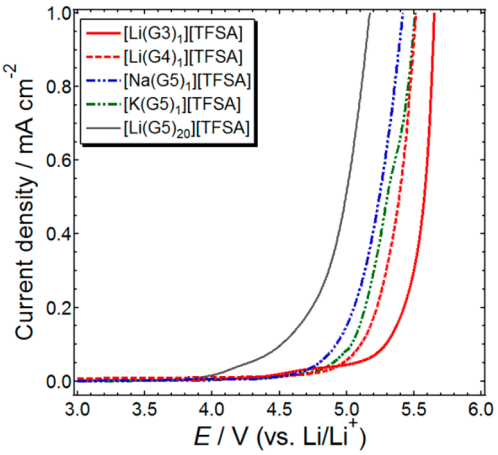

Figure 8. LSV curves of a series of $[M(glyme)_1][TFSA]$ complexes obtained at a scan rate of 1 mV s^{-1} at 60 °C. The curve of the G5−Li[TFSA] solution (i.e., $[Li(G5)_{20}][TFSA]$) is also included for comparison.

ether molecules are electrochemically oxidized at ∼4.0 V vs Li/Li^+. In fact, oxidative decomposition of $[Li(G5)_{20}][TFSA]$, which contains a large amount of excess (uncoordinating) glyme, starts at the electrode potential of 4.0 V vs Li/Li^+. In sharp contrast, the anodic limits of the studied solvate ILs are higher than ∼4.5 V vs Li/Li^+, which is consistent with previous reports.[18,35] As stated above, the strong electric field of M^+ ion polarizes the glyme oxygen atoms through complexation and thereby lowers the HOMO energy level of the glyme. In addition, free (uncoordinating) glyme molecules scarcely exist even in the molten state for good solvate ILs, as proven by phase-state-dependent Raman spectra and isothermal stability measurements. Therefore, complexation in a 1:1 ratio effectively enhances the oxidative stability of glymes.

As shown in Figure 8, the anodic limits obviously depend on the compositions of the molten complexes. To discuss the oxidative stability of the complexes in further detail, variations in the HOMO energy levels through complexation were evaluated via ab initio molecular orbital calculations based on the optimized structures. The calculated HOMO energy levels for pure glymes (all trans conformations), complex cation $[M(glyme)_1]^+$, and complex ion pair $[M(glyme)_1][TFSA]$ are listed in Table 2. The HOMO energy levels of pure G3, G4,

Table 2. HOMO Energy Levels of Glymes Calculated by HF/6-311G Level ab Initio Molecular Orbital Calculations**

sample	au	eV	ΔeV[a]
G3 (all trans)	−0.420 93	−11.45	0
$[Li(G3)_1]^+$	−0.575 52	−15.66	−4.21
$[Li(G3)_1][TFSA]$	−0.444 51	−12.10	−0.65
G4 (all trans)	−0.421 16	−11.46	0
$[Li(G4)_1]^+$	−0.556 25	−15.14	−3.68
$[Li(G4)_1][TFSA]$	−0.433 8	−11.80	−0.34
$[Na(G4)_1]^+$	−0.551 42	−15.00	−3.54
$[Na(G4)_1][TFSA]$	−0.437 77	−11.91	−0.45
G5 (all trans)	−0.421 33	−11.46	0
$[Na(G5)_1]^+$	−0.544 21	−14.81	−3.35
$[Na(G5)_1][TFSA]$	−0.440 36	−11.98	−0.52
$[K(G5)_1]^+$	−0.538 62	−14.66	−3.20
$[K(G5)_1][TFSA]$	−0.435 24	−11.84	−0.38

[a] ΔeV is the change in the HOMO level upon complexation from that of the isolated all-trans glymes.

and $[Li(G3 \text{ or } G4)_1][TFSA]$ are reproduced from ref 18. Although LSV measurements on $[Na(G4)_1][TFSA]$ could not be carried out due to its high melting point (71.9 °C); the calculated results are also summarized in order to survey the effect of the metal species on the HOMO energy level.

From the calculated results, the HOMO energy levels of $[M(glyme)_1]^+$ are lower than those of pure glymes, irrespective of both the metal species and glyme length; however, the magnitude of the reduction of the HOMO energy levels upon complexation is strongly dependent on the metal ion species in the following order: $Li^+ > Na^+ > K^+$. This result is attributed to the stronger electric fields induced by smaller cations. The HOMO energy levels of $[M(glyme)_1][TFSA]$, which is an ion pair complex, are higher than those of $[M(glyme)_1]^+$ owing to partial relaxation of the electric field induced by the Mi^+ ions because of the negative charge of $[TFSA]^-$ anions. However, the levels of the complex ion pairs are still lower than those of the corresponding pure glymes.

The ΔeV value of $[Li(G4)_1][TFSA]$ is lower than that of $[Na(G4)_1][TFSA]$, which is contrary to our expectations; this is likely due to the optimized structures used in the HOMO energy calculations. Table S3 in the Supporting Information summarizes the HOMO energy levels of the deformed glymes upon complexation. The initial structures of $[Li(G3)_1][TFSA]$ and $[Li(G4)_1][TFSA]$ are obtained from refs 18 and 51, respectively. As listed in the Supporting Information, Table S3, the HOMO energy levels of glymes strongly depend on the

DOI: 10.1021/jp508100s
J. Phys. Chem. B 2015, 119, 1523−1534

conformation, i.e., the optimized structures. Because coordinating glyme molecules possess high conformational flexibility, they can coordinate to metal ions in various different configurations. In addition, the coordinating states of glymes easily change in the liquid state because of the low energy barrier among them. The HOMO energy levels are calculated based on a specific static state; hence, it is difficult to take into account the dynamic coordination change. Furthermore, the differences in the electric-field effects of Li^+, Na^+, and K^+ ions are less noticeable, i.e., within ~±0.2 eV. Therefore, the HOMO energy calculations are not always effective for comparing the electric-field effect of metal ions on the actual oxidative stability of $[M(glyme)_1][TFSA]$. However, the calculations rationally account for the enhancement of the oxidative stability of glymes upon complexation; this consistency also supports the fact that the complex structures of $[M(glyme)_1]^+$ and/or $[M(glyme)_1][TFSA]$ are retained even in the liquid state.

The solvate structure can also affect the oxidative stability because the HOMO energy levels of coordinating glymes are sensitive to the coordination manner. In fact, the low stability of $[Li(G4)_1][TFSA]$ compared to that of $[Li(G3)_1][TFSA]$ appears to be caused by the coordination state of G4, where one oxygen atom within G4 is weakly bound (or unbound) with the Li^+ ion.[18,51] The LSV curves of $[Na(G5)_1][TFSA]$ and $[K(G5)_1][TFSA]$ indicate that the Na^+ complex is less stable than the K^+ complex toward electrochemical oxidation (Figure 8); nevertheless, the electric-field effect of Na^+ is stronger than that of K^+. As reported previously, G5 coordinates to the Na^+ ion in a characteristic manner,[20] whereas the K^+ ion is coordinated by G5 in a proper fashion, similar to that in the $[K(18C6)_1]^+$ cation. The difference in the coordination manner of G5 in $[Na(G5)_1][TFSA]$ and $[K(G5)_1][TFSA]$ is possibly a factor that imparts the evident result.

Thermal Stability. Temperature-dependent TG measurements were performed to evaluate the thermal stability of each good solvate IL. To clarify the effect of complexation on thermal stability, differences in the thermal-decomposition temperatures (ΔT_d) of $[M(glyme)_1][TFSA]$ and the corresponding glymes are shown in Figure 9. T_d is defined as the temperature at which a 5% loss of weight is observed. The T_d values of pure G3, G4, and G5 are 104.4, 134.1, and 175.7 °C, respectively. Figure 9 clearly illustrates that complexation of glymes with alkali-metal ions strongly inhibits evaporation of the coordinating glymes and ΔT_d depends on both the glyme length and metal ion species.

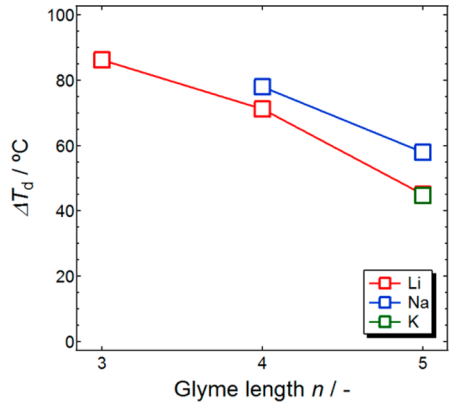

Figure 9. ΔT_d of a series of $[M(glyme)_1][TFSA]$ solvate ILs.

As shown in Figure 9, the ΔT_d values decrease with increasing coordinating glyme length, irrespective of the metal species. As stated before, weight loss in these systems occurs because of evaporation of desolvated glyme. While the stabilization energy for the complexation of M^+ with glymes increases with increasing glyme length,[51] the interaction energy between the M^+ ion and a single oxygen atom (M^+-O_{atom}) follows the opposite order; namely, longer glymes lead to weaker M^+-O_{atom} interactions. Because the last M^+-O_{atom} bond-cleavage process dominates the desolvation of glyme from $[M(glyme)_1]^+$ cations, complexation of M^+ ions with longer glymes results in smaller ΔT_d values than complexation with shorter glymes. On the other hand, the ΔT_d values for a series of equimolar complexes with the same ligand, e.g., G5, decrease in the following order: $[Na(G5)_1][TFSA] > [Li(G5)_1][TFSA] \approx [K(G5)_1][TFSA]$. Interestingly, equimolar complexes involving Na^+ ions always possess higher thermal stability than those involving Li^+ ions. In general, the M^+–glyme interaction strengthens with decreasing metal ion size because of the higher charge density of the metal ions. However, the ΔT_d results for $[Na(G5)_1][TFSA]$ are not completely explained by M^+–glyme interactions. Because there is competition between the ligands and $[TFSA]^-$ anions for interaction with the M^+ ions, the effect of the ion–ion ($M^+-[TFSA]^-$) interactions on the M^+–glyme interactions should also be considered. $M^+-[TFSA]^-$ interactions relax the positive charge on the M^+ ion; hence, stronger $M^+-[TFSA]^-$ interactions could lead to weaker M^+–glyme interactions, i.e., lower stability in complexes. The $M^+-[TFSA]^-$ interaction is closely related to the stabilization energies of the formation of ion pairs (complexes) (E_{form}) of the parent salts. Optimized structures of these salts have been reported previously and are reproduced in the Supporting Information, Figure S11.[66] The E_{form} values are −137.2, −110.5, and −101.1 kcal mol^{-1} for Li[TFSA], Na[TFSA], and K[TFSA], respectively, at the MP2/6-311G** level. The order of the E_{form} values agrees well with that of the ionic radii of the metal ions. The strong $Li^+-[TFSA]^-$ interactions cause weak Li^+–glyme interactions and, in consequence, the relatively low thermal stability of $[Li(glyme)_1][TFSA]$. On the other hand, in the case of $[K(G5)_1][TFSA]$, the intrinsically weak K^+–glyme interactions due to the low charge density of the K^+ ion probably causes this result, whereas the charge-screening effect on the K^+ ion due to the $M^+-[TFSA]^-$ interaction is the smallest among the studied congeners. A balance of these mutually competitive M^+–glyme and $M^+-[TFSA]^-$ interactions probably results in the specific stability of $[Na(glyme)_1][TFSA]$.

4. CONCLUSIONS

Comprehensive studies on a series of glyme–M[TFSA] binary mixtures were performed with respect to the solvate structures and stability. The compositions at which certain complexes were formed depended on both the glyme length and M^+ ion, and a trend in the complexation behavior of glymes with different M[TFSA] complexes was found. From isothermal stability measurements and phase-state-dependent Raman spectroscopy investigations on the mixtures, the structural criteria to achieve stable glyme–M[TFSA]-based complexes, namely good solvate ILs, were proposed; the criteria were primarily based on the coordination number of each metal ion.

The effect of the ion size on the electrochemical and thermal stabilities of the selected solvate ILs was examined. The improvement of oxidative stability upon complexation and

DOI: 10.1021/jp508100s
J. Phys. Chem. B 2015, 119, 1523−1534

anodic limits depended on the composition. The HOMO energy levels of coordinating glymes estimated by calculations partially corresponded to the experimental oxidative stability; however, those levels did not support the actual stability strictly because of the conformational diversity of the coordinating glymes in the molten state. Solvate ILs incorporating Na[TFSA] parent salts possessed higher thermal stabilities than those incorporating Li[TFSA] and K[TFSA] salts, irrespective of the glyme length. By considering the effect of the ion radii on the thermal stability, it was found that a balance among complicated competitive interactions determined the stabilities of the solvate ILs.

■ ASSOCIATED CONTENT

Supporting Information

Crystallographic data and thermal ellipsoid models for $[Li(G5)_1][TFSA]$, $[K(G5)_1][TFSA]$, $[Li(12C4)_1][TFSA]$, $[K(18C6)_1][TFSA]$, $[K(G4)_2]PF_6$, $[K(G5)_1]PF_6$, and $[K(G6)_1]PF_6$ are shown in Table S1 and Figures S1−S7, respectively. Selected $K-O_{glyme}$ distances are listed in Table S2. The HOMO energy levels of the deformed glymes are summarized in Table S3. Raman spectra of the crown-ether-based complexes (Figure S8) and $[Li(G2)_2][TFSA]$ (Figure S9), the relative intensity of the selected bands (Figure S10), and optimized structures of the parent M[TFSA] salts (Figure S11) are also included. The complete author list for ref 50 is given. Crystallographic data are given in CIF format. This material is available free of charge via the Internet at http://pubs.acs.org.

■ AUTHOR INFORMATION

Corresponding Author

*Tel.: +81-45-339-3955. Fax: +81-45-339-3955. E-mail: mwatanab@ynu.ac.jp.

Present Address

⊥T.M.: Department of Applied Physics, Chalmers University of Technology Göteborg, SE-412 96, Sweden.

Notes

The authors declare no competing financial interest.

■ ACKNOWLEDGMENTS

The authors thank Dr. Wesley A. Henderson for his significant suggestions on this study and kind support of our experiments. This study was supported in part by the Advanced Low Carbon Technology Research and Development Program (ALCA) of the Japan Science and Technology Agency (JST), the Technology Research Grant Program of the New Energy and Industrial Technology Development Organization (NEDO) of Japan, and the MEXT program "Elements Strategy Initiative to Form Core Research Center", Ministry of Education Culture, Sports, Science and Technology (MEXT) of Japan.

■ REFERENCES

(1) Tang, S.; Zhao, H. Glymes as versatile solvents for reactions and processes: from the laboratory to industry. *RSC Adv.* **2014**, *4*, 11251−11287.

(2) Pittman, C. U., Jr.; Yang, C. Dechlorination of polychlorobiphenyls using $NaBH_4$ and $NaBH_4$/LiCl at 120−310 °C in glyme solvents. *J. Hazard. Mater.* **2001**, *B82*, 299−311.

(3) Hogan, J. C.; Gandour, R. D. Structural Requirements for Glyme Catalysis in Butylaminolysis of Aryl Acetates in Chlorobenzene. Identification of $-OCH_2CH_2OCH_2CH_2OCH_2CH_2O-$ as the Optimal Subunit for Catalysis. *J. Org. Chem.* **1991**, *56*, 2821−2826.

(4) Ouchi, M.; Konda, M.; Nagamune, S.; Yoneda, A.; Hakushi, T.; Mishima, K. Solvent Extraction of Metal Picrates with Oligoethylene Glycol Glyme Derivatives. *Dev. Chem. Eng. Miner. Process.* **2003**, *11*, 481−490.

(5) Aurbach, D.; Granot, E. The study of electrolyte solutions based on solvents from the "glyme" family (linear polyethers) for secondary Li battery systems. *Electrochim. Acta* **1997**, *42*, 697−718.

(6) Xu, K. Nonaqueous Liquid Electrolytes for Lithium-Based Rechargeable Batteries. *Chem. Rev.* **2004**, *104*, 4303−4417.

(7) Slater, M. D.; Kim, D.; Lee, E.; Johnson, C. S. Sodium-Ion Batteries. *Adv. Funct. Mater.* **2013**, *23*, 947−958.

(8) Ryu, H.; Kim, T.; Kim, K.; Ahn, J.-H.; Nam, T.; Wang, G.; Ahn, H.-J. Discharge reaction mechanism of room-temperature sodium-sulfur battery with tetra ethylene glycol dimethyl ether liquid electrolyte. *J. Power Sources* **2011**, *196*, 5186−5190.

(9) Shao, Y.; Liu, T.; Li, G.; Gu, M.; Nie, Z.; Engelhard, M.; Xiao, J.; Lv, D.; Eang, C.; Zhang, J.-G.; Liu, J. Coordination Chemistry in megnesium battery electrolytes: how ligands affect their performance. *Sci. Rep.* **2013**, *3*, 3130 DOI: 10.1038/srep03130.

(10) Yin, Y.-X.; Xin, S.; Guo, Y.-G.; Wan, L.-J. Lithium-Sulfur Batteries: Electrochemistry, Materials, and Prospects. *Angew. Chem., Int. Ed.* **2013**, *52*, 13186−13200.

(11) Scheers, J.; Fantini, S.; Johansson, P. A review of electrolytes for lithium-sulfur batteries. *J. Power Sources* **2014**, *255*, 204−218.

(12) Dokko, K.; Tachikawa, N.; Yamauchi, K.; Tsuchiya, M.; Yamazaki, A.; Takashima, E.; Park, J.-W.; Ueno, K.; Seki, S.; Serizawa, N.; Watanabe, M. *J. Electrochem. Soc.* **2013**, *160*, A1304−A1310.

(13) Balaish, M.; Kraytsberg, A.; Ein-Eli, Y. A critical review on lithium-air battery electrolytes. *Phys. Chem. Chem. Phys.* **2014**, *16*, 2801−2822.

(14) Rahman, M. A.; Wang, X.; Wen, C. J. A review of high energy density lithium-air battery technology. *J. Appl. Electrochem.* **2014**, *44*, 5−22.

(15) Aurbach, D.; Gofer, Y.; Lu, Z.; Schechter, A.; Chusid, O.; Gizbar, H.; Cohen, Y.; Ashkenazi, V.; Moshkovich, M.; Turgeman, R.; Levi, E. A short review on the comparison between Li battery systems and rechargeable magnesium battery technology. *J. Power Sources* **2001**, *97*−*98*, 28−32.

(16) Tamura, T.; Yoshida, K.; Hachida, T.; Tsuchiya, M.; Nakamura, M.; Kazue, Y.; Tachikawa, N.; Dokko, K.; Watanabe, M. Physicochemical Properties of Glyme-Li Salt Complexes as a New Family of Room-temperature Ionic Liquids. *Chem. Lett.* **2010**, *39*, 753−755.

(17) Yoshida, K.; Tsuchiya, M.; Tachikawa, N.; Dokko, K.; Watanabe, M. Change from Glyme Solutions to Quasi-ionic Liquids for Binary Mixtures Consisting of Lithium Bis-(trifluoromethanesulfonyl)amide and Glymes. *J. Phys. Chem. C* **2011**, *115*, 18384−18394.

(18) Yoshida, K.; Nakamura, M.; Kazue, Y.; Tachikawa, N.; Tsuzuki, S.; Seki, S.; Dokko, K.; Watanabe, M. Oxidative-Stability Enhancement and Charge Transport Mechanism in Glyme-Lithium Salt Equimolar Complexes. *J. Am. Chem. Soc.* **2011**, *113*, 13121−13129.

(19) Ueno, K.; Yoshida, K.; Tsuchiya, M.; Tachikawa, N.; Dokko, K.; Watanabe, M. Glyme-Li Salt Equimolar Molten Mixtures: Concentrated Solution or Solvate Ionic Liquids? *J. Phys. Chem. B* **2012**, *116*, 11323−11331.

(20) Mandai, T.; Nozawa, N.; Tsuzuki, S.; Yoshida, K.; Ueno, K.; Dokko, K.; Watanabe, M. Phase Diagrams and Solvate Structures of Binary Mixtures of Glymes and Na Salts. *J. Phys. Chem. B* **2013**, *117*, 15072−15085.

(21) Angell, C.; Ansari, Y.; Zhao, Z. F. Ionic Liquids: Past, Present and Future. *Faraday Discuss.* **2011**, *154*, 9−27.

(22) Mandai, T.; Yoshida, K.; Ueno, K.; Dokko, K.; Watanabe, M. Criteria for Solvate Ionic Liquids. *Phys. Chem. Chem. Phys.* **2014**, *16*, 8761−8772.

(23) Seki, S.; Takei, K.; Miyashiro, H.; Watanabe, M. Physicochemical and Electrochemical Properties of Glyme-$LiN(SO_2F)_2$ Complex for Safe Lithium-ion Secondary Battery Electrolyte. *J. Electrochem. Soc.* **2011**, *158*, A769−A774.

DOI: 10.1021/jp508100s
J. Phys. Chem. B 2015, 119, 1523−1534

(24) Orita, A.; Kamijima, K.; Yoshida, M.; Dokko, K.; Watanabe, M. Favorable combination of positive and negative electrode materials with glyme-Li salt complex electrolytes in lithium ion batteries. *J. Power Sources* **2011**, *196*, 3874−3880.
(25) Yoshida, K.; Tsuchiya, M.; Tachikawa, N.; Dokko, K.; Watanabe, M. Correlation between Battery Performance and Lithium Ion Diffusion in Glyme-Lithium Bis(trifluoromethanesulfonyl)amide Equimolar Complexes. *J. Electrochem. Soc.* **2012**, *159*, A1005−A1012.
(26) Tachikawa, N.; Yamauchi, K.; Takashima, E.; Park, J.-W.; Dokko, K.; Watanabe, M. Reversibility of electrochemical reactions of sulfur supported on inverse opal carbon in glyme-Li salt molten complex electrolytes. *Chem. Commun.* **2011**, *47*, 8157−8159.
(27) Tatara, R.; Tachikawa, N.; Kwon, H.-M.; Ueno, K.; Dokko, K.; Watanabe, M. Solvate Ionic Liquid, $[Li(triglyme)_1][NTf_2]$, as Electrolyte for Rechargeable Li/Air Battery: Discharge Depth and Reversibility. *Chem. Lett.* **2013**, *42*, 1053−1055.
(28) Terada, S.; Mandai, T.; Nozawa, R.; Yoshida, K.; Ueno, K.; Tsuzuki, S.; Dokko, K.; Watanabe, M. Physicochemical Properties of Pentaglyme-Sodium Bis(trifluoromethanesulfonyl)amide Solvate Ionic Liquid. *Phys. Chem. Chem. Phys.* **2014**, *16*, 11737−11746.
(29) Choquette, Y.; Brisard, G.; Parent, M.; Brouillette, D.; Perron, G.; Desnoyers, J. E.; Armand, M.; Gravel, D.; Slougi, N. Sulfamides and Glymes as aprotic Solvents for Lithium Batteries. *J. Electrochem. Soc.* **1998**, *145*, 3500−3507.
(30) Brouillette, D.; Irish, D. E.; Taylor, N. J.; Perron, G.; Odziemkowski, M.; Desnoyers, J. E. Stable Solvates in Solution of Lithium Bis(trifluoromethanesulfonyl)imide in Glymes and Other Aprotic Solvents: Phase Diagrams, Crystallography and Raman Spectroscopy. *Phys. Chem. Chem. Phys.* **2002**, *4*, 6063−6071.
(31) Henderson, W. A.; McKenna, F.; Khan, M. A.; Brooks, N. R.; Young, V. G., Jr.; Frech, R. Glyme-Lithium Bis(trifluoromethanesulfonyl)imide and Glyme-Lithium Bis(perfluoroethanesulfonyl)imide Phase Behavior and Solvate Structures. *Chem. Mater.* **2005**, *17*, 2284−2289.
(32) Henderson, W. A.; Brooks, N. R.; Brennessel, W. W.; Young, V. G., Jr. Triglyme−Li^+ Cation Solvate Structures: Models for Amorphous Concentrated Liquid and Polymer Electrolytes (I). *Chem. Mater.* **2003**, *15*, 4679−4684.
(33) Henderson, W. A.; Brooks, N. R.; Young, V. G., Jr. Tetraglyme−Li^+ Cation Solvate Structures: Models for Amorphous Concentrated Liquid and Polymer Electrolytes (II). *Chem. Mater.* **2003**, *15*, 4685−4690.
(34) Henderson, W. A. Glyme−Lithium Salt Phase Behavior. *J. Phys. Chem. B* **2006**, *110*, 13177−13183.
(35) Papperfus, T. M.; Henderson, W. A.; Owens, B. B.; Mann, K. R.; Smyrl, W. H. Complexes of Lithium Imide Salts with Tetraglyme and Their Polyelectrolyte Composite Materials. *J. Electrochem. Soc.* **2004**, *151*, A209−A215.
(36) Hayamizu, K.; Akiba, E.; Bando, T.; Aihara, Y. ^1H, ^7Li, and ^{19}F Nuclear Magnetic Resonance and Ionic Conductivity Studies for Liquid Electrolytes Composed of Glymes and Polyetheneglycol Dimethyl Ethers of $CH_3O(CH_2CH_2O)nCH_3$ (n = 3−50) Doped with $LiN(SO_2CF_3)_2$. *J. Chem. Phys.* **2002**, *117*, 5929−5939.
(37) Grondin, J.; Lassègues, J.-L.; Chami, M.; Servant, L.; Talaga, D.; Henderson, W. A. Raman Study of Tetraglyme-$LiClO_4$ Solvate Structures. *Phys. Chem. Chem. Phys.* **2004**, *6*, 4260−4267.
(38) Zhang, C.; Ainsworth, D.; Andreev, Y. G.; Bruce, P. G. Ionic Conductivity in the Solid Glyme Complexes $[CH_3O(CH_2CH_2O)_nCH_3]$:$LiAsF_6$ (n = 3, 4). *J. Am. Chem. Soc.* **2007**, *129*, 8700−8701.
(39) Rhodes, C. P.; Frech, R. Local Structures in Crystalline and Amorphous Phases of Diglyme−$LiCF_3SO_3$ and Poly(ethylene oxide)−$LiCF_3SO_3$ Systems: Implications for the Mechanism of Ionic Transport. *Macromolecules* **2001**, *34*, 2660−2666.
(40) Zhang, C.; Lilly, S. J.; Ainsworth, D.; Staunton, E.; Andreev, Y. G.; Slawin, A. M. Z.; Bruce, P. G. Structure and Conductivity of Small-Molecule Electrolytes $[CH_3O(CH_2CH_2O)_nCH_3]$:$LiAsF_6$ (n = 8−12). *Chem. Mater.* **2008**, *20*, 4039−4044.
(41) Ueno, K.; Park, J.-W.; Yamazaki, A.; Mandai, T.; Tachikawa, N.; Dokko, K.; Watanabe, M. Anionic Effects on Solvate Ionic Liquid Electrolytes in Rechargeable Lithium−Sulfur Batteries. *J. Phys. Chem. C* **2013**, *117*, 20509−20516.
(42) Zhang, C.; Ueno, K.; Yamazaki, A.; Yoshida, K.; Mandai, T.; Umebayashi, Y.; Dokko, K.; Watanabe, M. Chelate Effects in Glyme/Lithium Bis(trifluoromethanesulfonyl)amide Solvate Ionic Liquids. I. Stability of Solvate Cations and Correlation with Electrolyte Properties. *J. Phys. Chem. B* **2014**, *118*, 5144−5153.
(43) Zhang, C.; Yamazaki, A.; Murai, J.; Park, J.-W.; Mandai, Y.; Ueno, K.; Dokko, K.; Watanabe, M. Chelate Effects in Glyme/Lithium Bis(trifluoromethanesulfonyl)amide Solvate Ionic Liquids, Part II: Importance of Solvate-Structure Stability for Electrolytes of Lithium Batteries. *J. Phys. Chem. C* **2014**, *118*, 17362−17373.
(44) Pederson, C. J. Cyclic Polyethers and Their Complexes with Metal Salts. *J. Am. Chem. Soc.* **1967**, *88*, 7017−7036.
(45) Dillon, R. E. A.; Shriver, D. F. Influence of Cation Size on Ionic Glass Formation and Ionic Conductivity. *Solid State Ionics* **2000**, *132*, 93−99.
(46) Hagiwara, R.; Tamaki, K.; Kubota, K.; Goto, T.; Nohira, T. Thermal Properties of Mixed Alkali Bis(trifluoromethylsulfonyl)-amides. *J. Chem. Eng. Data* **2008**, *53*, 355−358.
(47) Altomare, A.; Cascarano, G.; Giacovazzo, C.; Guagliardi, A.; Burla, M. C.; Polidori, G.; Camalli, M. *SIR92*—a Program for Automatic Solution of Crystal Structures by Direct Methods. *J. Appl. Crystallogr.* **1994**, *27*, 435.
(48) Sheldrick, G. M. *Program for the Refinement of Crystal Structures, SHELX97*; University of Göttingen: Göttingen, Germany, 1997.
(49) Sheldrick, G. M. A short history of SHELX. *Acta Crystallogr.* **2008**, *A64*, 112−122.
(50) Frisch, M. J.; Trucks, G. W.; Schlegel, H. B.; Scuseria, G. E.; Robb, M. A.; Cheeseman, J. R.; Montgomery, J. A., Jr.; Vreven, T.; Kudin, K. N.; Burant, J. C.; et al. *Gaussian 03*, revision E.01; Gaussian, Inc.: Wallingford, CT, 2004.
(51) Tsuzuki, S.; Shinoda, W.; Seki, S.; Umebayashi, Y.; Yoshida, K.; Dokko, K.; Watanabe, M. Intermolecular Interactions in Li^+-glyme and Li^+-glyme-$TFSA^-$ Complexes: Relationship with Physicochemical Properties of [Li(glyme)][TFSA] Ionic Liquids. *ChemPhysChem* **2013**, *14*, 1993−2001.
(52) Gjikaj, M.; Adam, A. Complexation of Alkali Triflates by Crown Ethers: Synthesis and Crystal Structure of $[Na(12\text{-crown-}4)_2][SO_3CF_3]$, $[Na(15\text{-crown-}5)][SO_3CF_3]$, $[Rb(18\text{-crown-}6)][SO_3CF_3]$, and $[Cs(18\text{-crown-}6)][SO_3CF_3]$. *Z. Anorg. Allg. Chem.* **2006**, *632*, 2475−2480.
(53) Mason, E.; Eick, H. A. Structure of a 1:2 complex of sodium perchlorate and 1,4,7,10-tetraoxacyclododecane (12-crown-4). *Acta Crystallogr., Sect. B: Struct. Crystallogr. Cryst. Chem.* **1982**, *38*, 1821−1823.
(54) Turner, D. R.; Pek, S. N.; Batten, S. R. Amide-water hydrogen-bond motifs in alkali-metal/crown ether complexes of carbamoyldicyanomethanide, $C(CONH_2)CN^-$. *New J. Chem.* **2008**, *32*, 719−726.
(55) Alexander, J. S.; Allis, D. G.; Teng, W.; Senge, K. R. Alkali Metal Diphenylmethanides: Synthetic, Computational, and Structural Studies. *Chem.—Eur. J.* **2007**, *13*, 9899−9911.
(56) Dillon, R. E. A.; Stern, C. L.; Shriver, D. F. Structural Comparisons of Fast Ion Conductors Consisting of $Li[(CF_3SO_2)_2N]$ Complexes with Cryptands or Crown Ether. *Solid State Ionics* **2000**, *133*, 247−255.
(57) Bock, H.; Sievert, M.; Bogdan, C. L.; Kolbesen, B. O.; Wittershagen, A. Biphenylene Ring Expansion by a $(H_3C)_2Si$ Link from Silicone Grease as Proven by the Crystal Structures of [(Sodium$^+$[2,2,1]cryptand) (9,9-dimethylsilafluorene$^{\bullet-}$)] as Well as [Sodium$^+$(triglyme)$_2$(biphenylene$^{\bullet-}$)] and by Total-Reflection X-ray Fluorescence Spectroscopy (TXRF). *Organometallics* **1999**, *18*, 2387−2389.
(58) Henderson, W. A.; Brooks, N. R.; Brennessel, W. W.; Young, V. G., Jr. $LiClO_4$ Electrolyte Solvate Structures. *J. Phys. Chem. A* **2004**, *108*, 225−229.

DOI: 10.1021/jp508100s
J. Phys. Chem. B 2015, 119, 1523−1534

(59) Seo, D. M.; Boyle, P. D.; Henderson, W. A. Poly[bis(acetonitrile-κN)bis[μ_3-bis(trifluoromethanesulfonyl)imido-$\kappa^4 O,O':O'':O'''$]dilithium]. *Acta Crystallogr.* **2011**, *E67*, m534.
(60) Yokota, Y.; Young, V. G., Jr.; Verkade, J. G. The homoleptic lithium complex $[Li(CH_3CN)_4]ClO_4$. *Acta Crystallogr.* **1999**, *C55*, 196−198.
(61) Sazama, G. T.; Betley, T. A. Ligand-Centered Redox Activity: Redox Properties of 3d Transition Metal Ions Ligated by the Weak-Field Tris(pyrrolyl)ethane Trianion. *Inorg. Chem.* **2010**, *49*, 2512−2524.
(62) Serrano, C. B.; Less, R. J.; McPartlin, M.; Naseri, V.; Wright, D. S. The First-Row Transition Metal Interstitial Hydride Anion $[\{PhP(CH_2)_3Fe\}_4(\mu_4\text{-}H)]^-$. *Organometallics* **2010**, *29*, 5754−5756.
(63) Zavalij, P. Y.; Yang, S.; Whittingham, M. S. Structural chemistry of new lithium bis(oxalato)borato solvates. *Acta Crystallogr.* **2004**, *B60*, 716−724.
(64) Herstedt, M.; Smirnov, M.; Johansson, P.; Chami, M.; Grondin, J.; Servant, L.; Lassègues, J. C. Spectroscopic characterization of the conformational states of the bis(trifluoromethanesulfonyl)imide anion ($TFSI^-$). *J. Raman Spectrosc.* **2005**, *36*, 762−770.
(65) Seo, D. M.; Borodin, O.; Han, S.-D.; Boyle, P. D.; Henderson, W. A. Electrolyte Solvation and Ionic Association II. Acetonitrile-Lithium Salt Mixtures: Highly Dissociated Salts. *J. Electrochem. Soc.* **2012**, *159*, A1489−A1500.
(66) Tsuzuki, S.; Kubota, K.; Matsumoto, H. Cation and Anion Dependence of Stable Geometries and Stabilization Energies of Alkali Metal Cation Complexes with FSA^-, FTA^-, and $TFSA^-$ Anions: Relationship with Physicochemical Properties of Molten Salts. *J. Phys.Chem. B* **2013**, *117*, 16212−16218.

DOI: 10.1021/jp508100s
J. Phys. Chem. B 2015, 119, 1523−1534